Structural Changes and Reactivity of Hematite Subjected to Extended Milling

P. Pourghahramani, E. Forssberg

Mining Engineering Department, Sahand University of Technology, Tabriz, Iran

Email: pourghahramani@sut.ac.ir

ABSTRACT

Several structural characteristics change during intensive milling such as chemical composition, phase transformation, crystallite size, lattice strain, lattice parameter (s) and solid reactivity etc. The creation of defects enhances the stored energy (enthalpy) in the solids and consequently causes a decrease of activation barrier for the process and/or subsequent processes.

In this paper, the effects of milling on the structural changes of hematite have been investigated using dry millings. The structural changes have been characterized using a combination analysis of BET surface area measurements and X-ray diffraction (XRD) analysis. Besides, the hydrogen reduction behaviors and kinetics of mechanically activated samples and initial sample were studied using simultaneous thermal analysis (STA). The methods of Williamson-Hall and Warren-Averbach were used for analyzing of XRD patterns to resolve and extract the microstructural characteristics of hematite phases.

It was concluded that the breakage and aggregation of particles take place mainly in the starting and prolonged stages of dry grinding, respectively. The BET surface area enlarged steadily over the grinding processes whatever milling methods were utilized. The characterization of structural changes revealed that the hematite milled under various conditions did not undergo any significant reaction or phase transformation during milling processes. In addition, X-ray amorphous phase content increased gradually with extending the grinding intensity. The maximum X-ray amorphous phase exceeds about 81% after 9 hours of milling in both tumbling mill and vibratory mill. The Williamson-Hall plots revealed the anisotropic character of line broadening for deformed hematite and changes in the trend of microstructural characteristics as a function of milling time. It was found that the surface weighted crystallite size decreases and lattice strain increases over the grinding periods. The minimum surface weighted crystallites were calculated about 17.3 nm, 12.2 nm for the products of tumbling and vibratory mills respectively. The maximum lattice strain, $<\varepsilon^2_{L=10\text{nm}}>^{1/2}$, in the grinding with tumbling and vibratory mills was calculated about 4.44×10^{-3} and 3.95×10^{-3} respectively.

The non-isothermal kinetic analysis of the products revealed that Fe_2O_3 reduced to Fe in a two-step process via Fe_3O_4. Intensive grinding resulted in improved resolution of overlapping reduction events. It was also established that the mechanical activation had a positive effect on the first step of reduction. The prereduction step in the activated samples initiated and completed at lower temperatures than that in non-activated samples. The activation energy of reduction decreased at the first step of reaction with increasing the grinding intensity. Intensive milling increased slightly the average activation energy of the second step of reduction due to the present of finely agglomerated particles and intensive sintering of the particles in higher temperature ranges.

Keywords: Mechanical activation; Extended grinding; Microstructure; Hematite; Reduction kinetics

INTRODUCTION

Mechanical activation (MA), a narrow field of the Mechanochemistry (MC) applied for the activation of chemical reaction by mechanical

energy, has been used in mineral processing to produce finely ground particles, increased surface area and improved chemical reactivity of milled materials. The process involves prolonged grinding and is reported to cause a variety of processes to take place such as generation of a large new surface, formation of dislocations and point defects in the crystalline structure, phase transformations in polymorphic materials, chemical reactions, decomposition, ionic exchange, and oxidation and reduction reactions.

The active mechanical energy is partially transferred to the particles, e.g. by the impact of solid particles or by induction of tensile and compressive forces in powder mass. The influence of mechanical energy on solids includes a multitude of elementary physicochemical micro and macroprocesses. The mechanical energy leads to changes of the material structure, to the occurrence of structural defects such as changes of the surface, lattice distortion and conversion of long range order to short range order. Therefore, the free energy or chemical potential gained and the composition can change during the mechanical activation. In this way the solid systems reach an activated state (Baláž, 2000; Tkáčová, 1989).

On the other hand, mechanical activation of solid substances is one component of modern scientific disciplines of mechanochemistry. At present, mechanical activation exhibits a wide range of application potential. It has been reported that mechanical activation substantially accelerates the leaching kinetics of several sulfide and oxide minerals, even at ambient pressure. The enhanced effect is attributed to the increase of specific surface area and structural disorder (Baláž, 1996), enhanced strain (Baláž, 2000), amorphization of mineral particles (Tkáčová et al., 1993), preferential dissolution of select crystal faces (Barton et al., 1979), microtopography (Tromans and Meech, 1999), and formation of new phases more amenable to leaching (Welham, 2001). Mechanical activation was also established to be successful for intensification of the thermal processes of sulfide minerals, such as oxidation, decomposition in inert atmosphere, and sublimation (Tkáčová et al., 1990). Hu et al. (2002, 2003) reported that mechanically activated pyrite and galena are more easily decomposed during thermal treatments than non-activated pyrite and galena. Recently, the effect of extended milling on carbothermic reduction of ore manganese was investigated by Welham (2002). Milling of manganese ore with graphite led to enhanced reduction at decreased temperatures. The study of carbothermic reduction hematite (mixture of hematite and graphite) in air revealed that milling at ambient temperature increases the rate of reaction (Raygan et al., 2002). In this area, thermal properties of mechanically activated hematite concentrate using simultaneous thermal analysis have yet to be studied.

The aim of the present paper is to investigate the influence of different experimental conditions and activation devices on hematite concentrate. In addition, the effects of mechanical activation on the thermal behavior and the reduction kinetics of mechanically activated hematite were investigated and described.

EXPERIMENTAL

Material

The high-purity hematite concentrate used in this study was kindly supplied by the LKAB (Luossavaara Kiirunavaara Aktiebolag) company in Sweden. The chemical analysis showed that the initial hematite powder contained about 97.91% Fe_2O_3, 0.73% Al_2O_3, 0.73% SiO_2, 0.26% TiO_2, 0.20% MgO, 0.022% MnO, and 0.088% P_2O_5. Other components such as K_2O, CaO and Na_2O comprise 0.051%. The X-ray diffraction analysis represented only the hematite diffraction peaks.

Mechanical activation and characterization

Hematite concentrate was mechanically activated using a tumbling mill and a vibratory mill. A mixture of ball steel media with dimensions between 6 mm and 22.2 mm and with apparent density of 4875 kg/m^3 was used as grinding media. The milling experiments were performed continuously in air atmosphere. The experimental milling conditions are given in Table 1. The activated samples were sealed into plastic tubes and kept in a freezer.

The particle size distribution of the samples was measured by laser diffraction (CILAS 1064) in the liquid mode, from which the granulometric surface areas were obtained. The specific surface area of the samples was determined by

Table 1 Experimental milling conditions and mill types

Milling conditions	Tumbling milling	Vibratory milling
Specific input energy/(kWh/kg)	0.1996-6.221	0.6~21.92
Media filling/%	38.9	70
Milling time/h	1, 3, 9	1, 3, 9
Ball to powder weight ratio	16.77:1, 67:1	16.92:1, 67.68:1
Speed/RPM	60	1000
Amplitude/mm	–	8
Media apparent density/(gr/cm^3)	4.875	4.875
Amplitude/mm	–	8
$L\times\phi$/mm	275 × 245	320 × 185

the BET method with the Flow Sorb II 2300 (Micromeretics).

The XRD patterns were obtained using a Siemens D5000 powder diffractometer with Bragg-Brentano geometry equipped with a curved graphite monochromator in the diffracted beam arm and using Cu Kα radiation (λ = 0.15406). To characterize the microstructural characteristics encountered during the mechanical activation of specimens, the line broadening analysis based on XRD pattern characteristics was applied. For interpreting of line broadening Williamson-Hall and Warren-Averbach methods were applied. The profile fitting procedure and principles of the methods were discussed in detail elsewhere (Pourghahramani and Forssberg, 2006 a, b).

Thermogravimetric analyses (TG) were conducted with a NETZSCH STA 409C instrument at three heating rates of 10°C·min^{-1}, 15°C·min^{-1} and 20°C·min^{-1} from room temperature to 850°C. The high temperature furnace was heated by graphite heating elements, which were protected by injection of inert argon gas. The temperature of furnace was controlled by a tungsten thermocouple. The heating was performed under highly pure hydrogen as reduction gas with a flow rate of 100 mL·min^{-1}. The mass of samples was almost 95 mg.

RESULTS AND DISCUSSION

Changes in the surface areas

The mechanical activation of materials is accompanied by disintegration and generation of fresh previously-unexposed surfaces. Fig. 1 shows how the BET surface area and granulometric surface area change with milling time in the mills. The most obvious shown feature is that the vibratory mill brings about higher specific surface area than the tumbling mill. Furthermore, the specific surface area in the initial

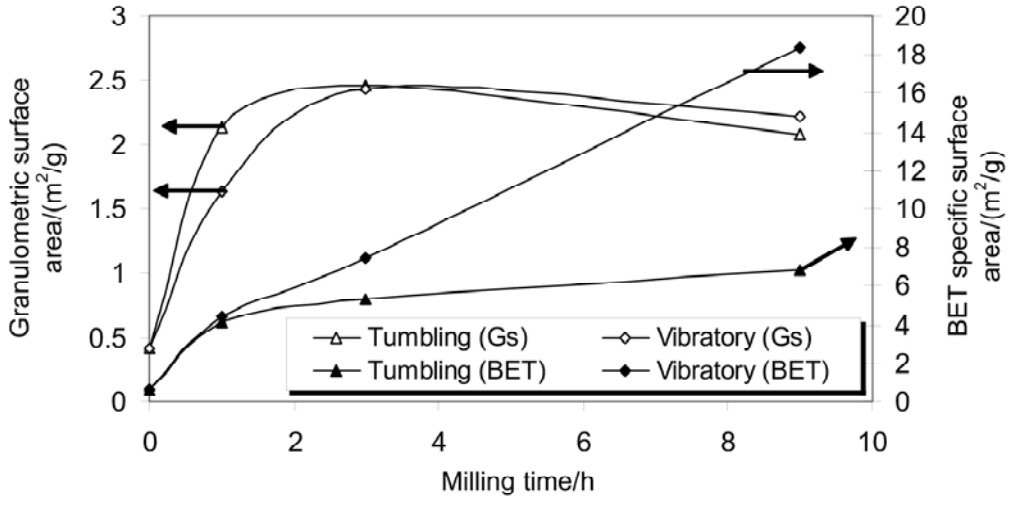

Fig. 1 Changes in the specific surface area and granulometric surface area of hematite ground in the mills as a function of grinding time

stages of grinding increases rather sharply and continues to rise gradually. However, the BET surface area in the products of the tumbling mill increases marginally in the prolonged milling in spite of the vibratory mill products, which continues to increase sharply. This may be related to the ability of vibratory milling to reduce particle size. After 9 hours of milling, the maximum specific surface area in the milling with vibratory mill and tumbling mill ranged to 6.8 m^2/g and 18.4 m^2/g respectively.

The granulometric surface areas of the samples are also compared in Fig. 1. With progress in the milling, the granulometric surface area shows increasing trend and then decreasing trend. From the decrease in the granulometric surface areas and the increase in the BET specific surface areas, the formation of aggregates among particles can be concluded. The agglomeration of the particles during extended dry]grinding was reported for sulphide minerals (Baláž, 2000), oxide minerals (Tkáčová, 1989) and olivine (Kleiv and Thornhill, 2006). This behavior is common for dry grinding and is usually explained by aggregation of the structurally modified particles following the initial reduction of particle size. This is because of the tendency of the activated material to reduce their surface free energy.

XRD pattern characteristics

Fig. 2 shows the XRD pattern of the initial sample and mechanically activated samples in the tumbling mill as a function of milling time. The diffraction peaks for mechanically-activated samples are lower and broader than of those for non-activated samples, mainly due to a disordering process of hematite crystal structure by intensive grinding. The reduction of diffraction peaks intensities implies the formation of amorphous material. The decrease of X-ray diffraction intensities is accompanied by a general broadening of the XRD patterns. The increase of the XRD line breadths is due to the plastic deformation and disintegration of hematite. The XRD patterns showed only the hematite reflections, indicating that hematite did not undergo significant reaction and phase changes. The presence of small, but remarkable, reflection peaks after intensive grinding in the grinding mills can be taken as a further indication of the high milling resistance and mechanical strength of the submicron hematite crystallites. Similar results were obtained for the samples ground by Vibratory mill.

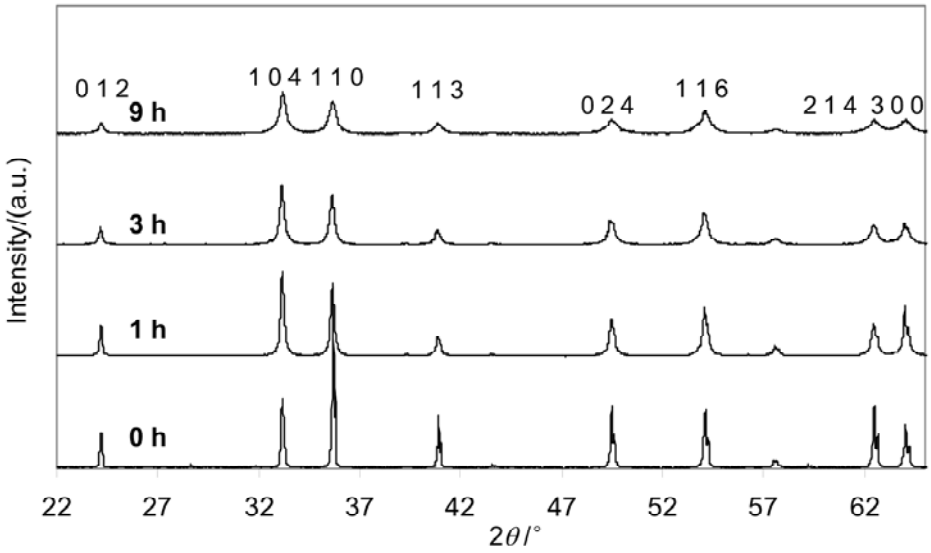

Fig. 2 XRD patterns of hematite samples ground in the tumbling mill as a function of the grinding time

X-ray amorphization degree

From the intensity of the reflection peaks and their background, the degree of X-ray amorphization is estimated and the results are depicted in Fig. 3. The content of X-ray amorphous phase in the hematite samples depends mainly on grinding time. The portion of X-ray amorphous phase in the ground hematite with the tumbling mill is slightly higher than of those ground in the vibratory mill. The fraction of the X-ray amorphization increases steadily with progress in milling. The amorphization degree increased to 81% after 9 hours of milling in the

mills. The increase of X-ray amorphous phase due to intensive milling was reported for calcite and quartz (Heegn, 1986) and sulphide minerals (Baláž, 2000). The amorphization is in fact a highly distorted periodicity of lattice elements, and it is often characterized as a short range order in contrast to the long order of a fully crystalline structure.

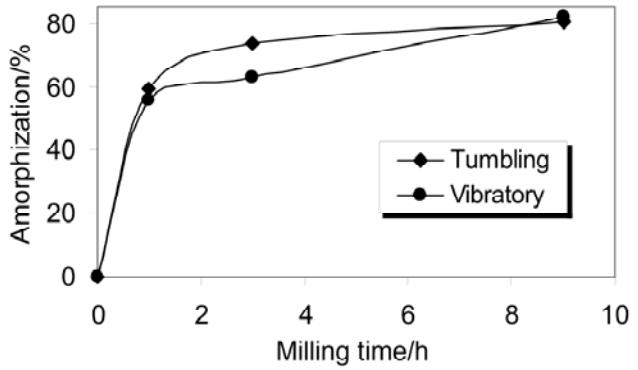

Fig. 3 Variation of X-ray amorphization degree with the time of mechanical activation in the mills

Microstructural characteristics

To obtain the microstructural characteristics, two methods including the simplified integral breadth and Warren-Averbach approach were used. The first step in analyzing line broadening is to ascertain the nature of any structural imperfections present. This can be achieved from the Williamson-Hall plots. Williamson and Hall (1953) proposed a method for resolving size and strain broadening. Williamson-Hall plots can be applied to a Gaussian profile (Santra et al., 2002).

$$\beta_f^{*2} = \left(\frac{\beta_f \cos\theta}{\lambda}\right)^2 = \frac{1}{D_v^2} + 4\varepsilon^2 d^{*2}$$

$$2\sin\theta/\lambda = 1/d = d^* \qquad (1)$$

where terms d and β_f refer to the interplanar spacing and measured (physical) broadening respectively. A plot of β_f^{*2} against $4d^{*2}$ give a straight line. The intercept and slope of line yield $(1/D_v)^2$ and ε^2, respectively. However, the qualitative results from Williamson-Hall method favor the quantitative results. Thus only the qualitative results are discussed below.

The Williamson-Hall plots are illustrated in Fig. 4 for all activated samples using vibratory mill. Similar results were obtained for the ground samples in the tumbling mill. The correlation coefficients were estimated between 0.8 and 0.97 depending on the sample. This indicates relatively a strong relationship between β_f^{*2} and d^{*2}. From the Williamson-Hall plots, lines for all intensive reflections and [012] direction have non-zero and different slopes and intercepts. This suggests that the strain and size contributions exist simultaneously in the milled samples. The increase of physical broadening vs. grinding time and indicates that intensive milling extends great defects and deformations in materials. The scatter of the β_f^{*2} values indicates that the crystallite shape differs from a spherical one. Besides, the (024) reflection shows higher deviation than other reflections and its broadening enlarged as the intensity of milling increased. There is also a systematic deviation between the line connecting the two orders of (012) and (024) reflections and the line connecting all intensive reflections, the line concerning to the [012] direction lie above it. This may be understood by considering the anisotropy in the elastic properties of the single-crystal hematite, indicating that hematite crystal is 'soft' between the (024) and the others crystallographic directions. The similar results have been observed for Fe powder (Borner and Eckert, 1997; Vives et al., 2004) and ball milled molybdenum powder (Lucks et al., 2004).

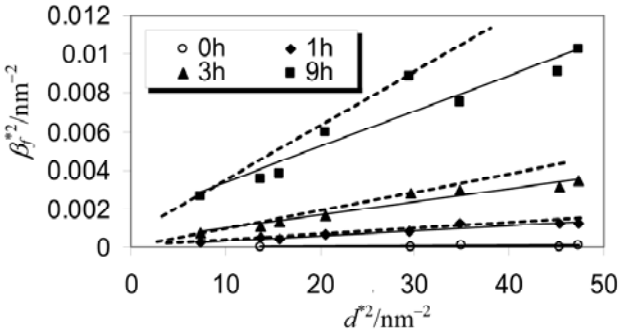

Fig. 4 Williamson-Hall plots, B_f^{*2} versus d^{*2}, for samples milled in the vibratory mill. The solid and dashed line refers to all intensive reflection peaks and direction [012] respectively.

The quantitative results concerning microstructure characteristics were obtained using Warren-Averbach method. The crystallite size quantity and the root mean square strain $< \varepsilon^2_{L=10\text{nm}} >^{1/2}$ are given in Table 2. The results depict the nature of progressive evolution of the microstructure of the milling products vs. grinding time. Generally, the surface-weighted crystallite size shows decreasing and root mean square strain ($< \varepsilon^2_{L=10} >^{1/2}$) increasing trend as

grinding time increases whatever mill used. In the earlier stages of milling, the crystallite size decreases rapidly to the nanometer range. Further refinement proceeds slowly and the final average grain size is in the order of 12~17 nm depending on the mill. As the intensity of milling increases, the ground hematite in tumbling mill yields more strain and larger crystallites than that of ground in vibratory mill. The steady state was not observed for grinding conditions, suggesting that the production of small crystallites is still possible with increasing the grinding intensity.

Table 2 The microstructural characteristics in [012] direction using the Warren-Averbach method for activated hematite in different environments. D_s and $<\varepsilon^2_{L=10nm}>^{1/2}$ indicate the surface weighted crystallite size and root mean square strain (RMSS) at L=10nm respectively

Milling type	Time/h	D_s/nm	$<\varepsilon^2_{L=10nm}>^{1/2}$ /$\times10^{-3}$
	1	44.4	2.236
Tumbling mill	3	25.0	2.84
	9	17.3	4.44
	1	36.4	1.84
Vibratory mill	3	23.7	2.79
	9	12.2	3.95
Initial hematite*	0	199.1	n. d. (0)

*Calculated using single peak method.

Reduction behavior

In order to obtain additional information about the weight loss of the sample obtained by milling, a TG analysis and a DTG analysis were performed. In these techniques, changes in the mass of a sample are studied while the sample is subjected to a controlled temperature program (Fig. 5). Generally, the TG curves for the reduction of hematite exhibit a two-step weight loss that can be identified from changes in the slope of the curves. The changes in the slope of the curves at weight loss 3.3% correspond to the quantitative conversion of hematite to magnetite. The total weight loss for all of the samples is 30%, which corresponds to the complete conversion of hematite to iron ($Fe_2O_3 \rightarrow Fe_3O_4 \rightarrow Fe$). For the ground hematite samples, the TG curves shift toward lower temperatures with increasing grinding time up to a temperature of about 640 ˚C. At low temperatures, the grinding time has a large effect on the weight loss, but its effect is limited with progress of reaction. At temperatures beyond 640˚C, reduction in the ground samples is delayed and no significant difference exists among the activated samples.

The DTG curves corresponding to the heating rate of 10 ˚C/min for the initial sample and the samples ground in the vibratory mill for different periods are shown in Fig. 5 as a function of temperature. The DTG curves also represent a two-step weight loss which can be easily identified from the changes in the slope and the peaks of the curves. The first step of weight loss, corresponding to the reduction of hematite

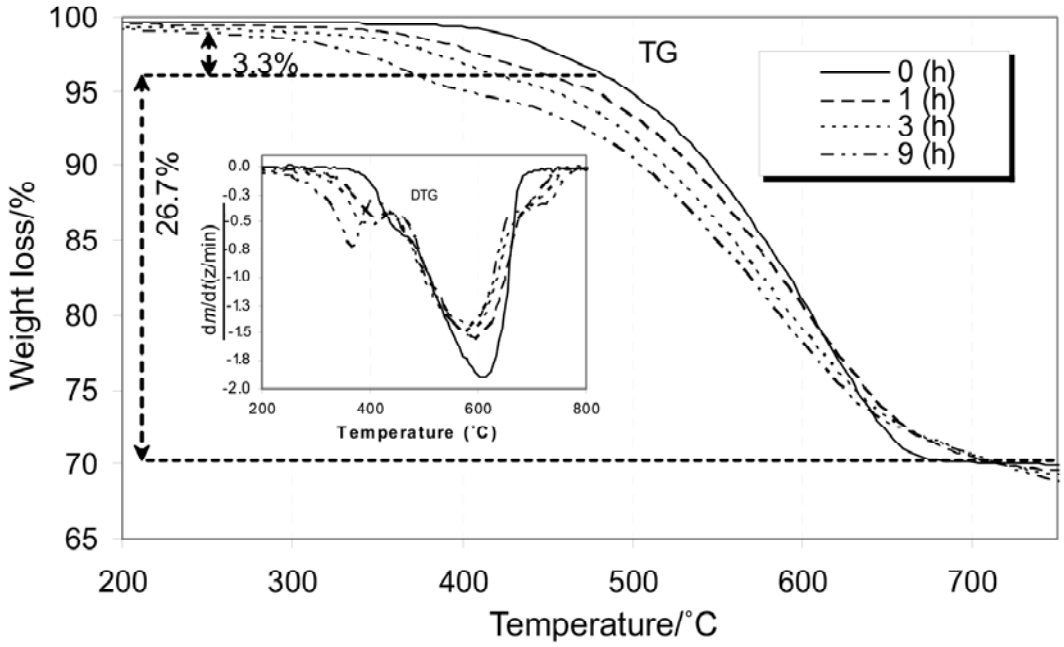

Fig. 5 TG and DTG curves (shown in the insets) for the initial sample and for samples ground in the vibratory mill as a function of temperature

to magnetite, occurs at the lower temperatures. The second step (main step) of weight loss, the reduction of magnetite to iron, extends toward higher temperature sides up to 700°C. It is apparent that the resolution of the two events is greater for mechanically activated samples than for the initial sample. This is a consequence of the reduction of the energy required to reorganize the crystalline structure of hematite. The energy supplied by milling causes structural disorder through the distortion or breakage of the crystalline network. This was evident from the reduction of the intensities of XRD peaks. Once more, this emphasizes that the mechanical activation results in improved resolution of overlapping reduction events. Moreover, the area of peak in the second step of reduction decreases concomitantly as the area of peak in the first weight loss step centered approximately between 300°C and 450°C increases, depending upon grinding time. For the non-activated hematite, the first step of reduction initiates and terminates at a certain temperature range. This is an expected property for crystalline hematite. However, activated hematite exhibits different starting and finishing temperatures of reduction in the first step of reduction, depending on grinding times and consequently the structural changes induced during milling.

Kinetic analysis

The isoconversional method of Kissinger-Akahira-Sunose (KAS) (1957) was used to determine the activation energy of the different reactions. The application of the isoconversional methods requires the determination of the absolute temperature at which a fixed extent of reduction from the several TG curves recorded at different heating rates. The degree of conversion between 0.02 and 0.95 is investigated. The dependence of the activation energy E on α characteristic for hydrogen reduction of non-activated hematite and mechanically activated hematite for different periods is shown in Fig. 6.

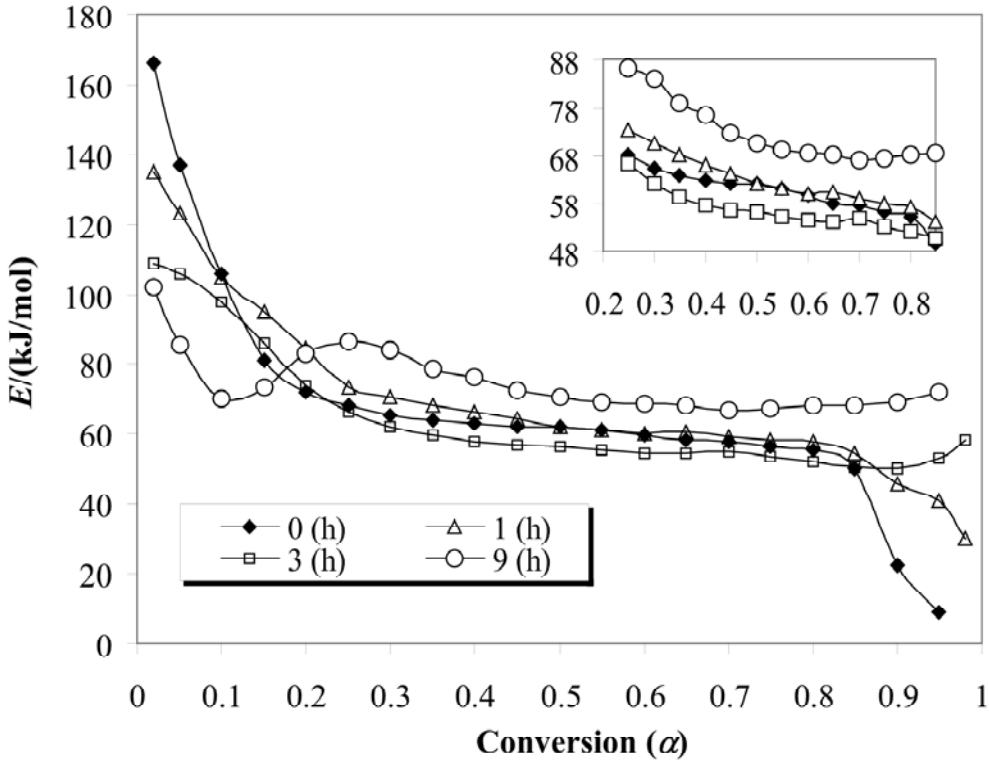

Fig. 6 Dependence of E_a on a characteristic of the reduction of non-activated hematite and mechanically activated hematite for various grinding times; a large scale of the curves for the range of $0.25 \leqslant \alpha \leqslant 0.85$ are shown in inset

The overall decreasing dependence of the activation energy on α indicates that the overall reaction contains at least two steps. A decrease in the activation energy is most likely caused by transition of the limiting step from the higher activation energy reaction to the lower activation energy reaction. The curves corresponding to the initial sample and the mechanically activated samples show that E decreases with extent of conversion (α) by $\alpha \leqslant 0.11$, corresponding

the reduction of hematite to magnetite, with increasing the grinding time. After this range, the activation energy continues to decrease for the initial sample and mechanically activated samples up to three hours as opposed with the activation energy for mechanically activated sample within 9 hours in which the activation energy tends to increase slightly and then decreases by $\alpha \leqslant 0.85$. The activation energy of the initial sample and ground sample for 1 hour decrease drastically when the conversion degree exceeds 0.85 as opposed with the reduction of the activated samples for more than 1 hour.

The first step of reduction, corresponding to $\alpha \leqslant 0.11$, in the initial sample describes with activation energy of about 106 ~ 166 kJ·mol^{-1}, while the calculated value for the second reduction step, corresponding to $0.11 < \alpha \leqslant 0.95$, is about 9 ~ 72 kJ·mol^{-1}. For activated hematite, the activation energy for the range of $\alpha \leqslant 0.11$ decreases with increasing grinding time. The activation energy from 106 ~ 166 kJ·mol^{-1} range in the initial sample decreases to about 70 ~ 102 kJ·mol^{-1} in the sample ground for 9 hours. The disordering of structure in mechanically activated samples brings about an increase in the rate of reduction process and a decrease in the activation energy (Baláž, 2000). For the second step of reduction, the ground sample up to one hour exhibits no significant difference in activation energy by conversion degree of 0.85. Grinding for three hours result in a slightly smaller activation energy compared with the initial sample; while prolonged milling for 9 hours leads to higher activation energy than the initial sample. This can be attributed to the agglomeration of finely ground particles during intensive milling and subsequently to the formation of a dense layer as a result of the partial sintering at higher temperatures. As a result, the effect of disordering of hematite structure overlapped by the formation of the dense layer. Therefore, the reduction is retarded (Pourghahramani and Forssberg, 2007). It can be concluded that mechanical activation has a positive effect on the prereduction step in terms of activation energy and small positive effect on the second step of reduction in the samples ground up to three hours.

Furthermore, the dependence of the apparent activation energy (E) on the extent of conversion (α) is a source of additional kinetic information of process (Vyazovkin and Wight, 1997). The curves obtained for non-activated sample and mechanically activated samples up to three hours reveal a typical reversible reaction according to Vyazovkin and Lesnikovich (1990). Vyazovkin and Linert (1995) have been shown that the decreasing dependence of E on α corresponds to the kinetic scheme of a reversible reaction followed by an irreversible one. For such process E is limited by the sum of the activation energy of the irreversible reaction and the enthalpy of the reversible reaction at low conversions. At high values of conversions, E is limited only by the activation energy of the irreversible reaction at high α. In our case, the reduction of hematite to magnetite probably proceeds through the exothermic stage at low conversion degrees, which is characterized by a high value of the apparent activation energy between 166 kJ/mol and 70 kJ/mol depending on the sample. The high values of the effective activation energy represent the sum of the enthalpy of the reversible process and of the apparent activation of the irreversible process. On the other hand, lower value of the activation energy at higher conversions is a characteristic of the process proceeding through a reversible endothermic process. For mechanically activated sample for 9 hours, the decreasing dependence of the activation energy is followed by increasing and then decreasing the activation energy for $\alpha \geqslant 0.11$; indicating increasing difficulty in the progress of reaction. The second step is probably involving competiting between the reduction of magnetite to iron and sintering process which may account for the increasing dependence of E on α.

CONCLUSIONS

From the study, it was concluded that the use of prolonged grinding caused great structural changes in the hematite structure. Mechanical activation led to higher specific surface area, X-ray amorphous material, microstrain, and smaller crystallites whatever milling types were applied. The aggregation of particles during extended dry milling occurs as result of the tendency of the activated material to reduce their surface free energy. After 9 hours of mill-

ing in tumbling and vibratory mills, the surface weighted crystallite size reached 17.3 nm and 12.2 nm respectively. The maximum lattice strain, $< \varepsilon^2_{L=10nm} >^{1/2}$, in the grinding with tumbling and vibratory mills was found about 4.44×10^{-3} and 3.95×10^{-3} respectively.

The reduction of Fe_2O_3 to Fe was found to occur in a two step process via Fe_3O_4. The TG and DTG analysis showed that the two reduction steps took place consecutively. The prereduction step in the activated samples initiated and completed at lower temperatures than that in non-activated samples. The activation energy of the first step of reduction decreased with increasing the grinding time. Intensive milling increased slightly the average activation energy of the second reduction step due to the present of finely agglomerated particles and probably intensive sintering of the particles in higher temperature ranges.

REFERENCES

Baláž, P, 2000. Extractive Metallurgy of Activated minerals (Elsevier, Amesterdam).

Barton, A F M and McConnel, S R, 1979. Rotating disc dissolution rates of ionic solids: Part 3. Natural and synthetic ilmenite. J. Chem. Soc, Faraday Trans. I 75: 971-983.

Borner, I and Eckert, J, 1997. Nanostructure formation and steady-state grain size of ball-milled iron powders. Mater. Sci. Eng. A 226-228: 541-545.

Heegn, H, 1986. Concerning some fundamentals of fine grinding. In: Leschonski, K., Editor, 1986. Proc. 1st World Congress on Particle Technology, Part II. Comminution 1986 (Nürnberger Messe und Austellungsgesellschaft, Nürnberg): 63-67.

Hu, H, Chen, Q, Yin, Z, Zhang, P and Ye, L, 2003. The thermal behavior of mechanically activated galena by thermogravimetry analysis, Metall. Mater. Trans. 34A: 793-797.

Hu, H, Chen, Q, Yin, Z, Zhang, P, Zou, J and Che, H, 2002. Study on the kinetics of thermal decomposition of mechanically activated pyrites, Thermochim. Acta 389: 79-83.

Kissinger, H E, 1957. Reaction kinetics in differential thermal Analysis, Anal. Chem. 29, 1702-1706

Kleiv, R A, and M. Thornhill, M, 2006. Mechanical activation of olivine, Minerals Engineering 19 (4): 340-347.

Lucks, I, Lamparter, P, and Mittemeijer, E J, 2004. An evaluation of methods of diffraction-line broadening analysis applied to ball-milled molybdenum. J. App. Cryst. 37: 300-311.

Pourghahramani, P and Forssberg, E, 2006a, Microstructure characterization of mechanically activated hematite using XRD line broadening, Int. J. Miner. Process.79: 106-119.

Pourghahramani, P and Forssberg, E, 2006b. Comparative study of microstructural characteristics and stored energy of mechanically activated hematite in different grinding environments, Int. J. Miner. Process.79: 120-139.

Pourghahramani, P and Forssberg, E, 2007, Effects of mechanical activation on the reduction behavior of hematite concentrate, Int. J. Miner. Process 82: 96-105.

Raygan, S, Khaki, J V, Aboutalebi, M R, 2002. Effect of mechanical activation on the packed-bed, high-temperature behavior of hematite and graphite mixture in air. J. Mater. Synth. Process. 10: 113-120.

Santra, K, Chatterjee, P, Sen and Gupta, S P, 2002. Voigt modeling of Size-Strain analysis: Application to $\alpha - Al_2O_3$ prepared by combustion technique. Bull. Mater. Sci., 25(3): 251-257.

Tiernan. M J, Barnes, P A, and Parkes, G M B, 2001. Reduction of iron oxide catalysts: the investigation of kinetic parameters using rate perturbation and linear heating thermoanalytical techniques, J. Phys. Chem., 105: 220-228.

Tkáčová, K, 1989. Mechanical Activation of Minerals (Elsevier, Amesterdam).

Tkáčová, K, Baláž, P and Bastl, Z, 1990. Thermal characterization of changes in structure and properties of chalcopyrite after mechanical activation, Thermochim. Acta 170: 277-287.

Tkáčová, K, Baláž, P, Mišura, B, Vigdergauz, V E and Chanturiya, V A, 1993. Selective leaching of zinc from mechanically activated complex Cu-Pb-Zn concentrate, Hydrometallurgy 33: 291-300.

Tromans, D and Meech, J A, 1999. Enhanced dissolution of minerals: Microtopography and mechanical activation, Miner. Eng. 12: 609-625.

Vives, S, Gaffet, E and Meunier, C, 2004. X-ray diffraction line profile analysis of Iron ball milled powders, Mater. Sci. Eng. A 366, 229-238.

Vyazovkin, S and Linert, W, 1995. Kinetic analysis of reversible thermal decomposition of solids, Int. J. Chem. Kinet. 27: 73-84.

Vyazovkin, S and Wight, C A, 1997. Kinetics in solids, Annu. Rev. Phys. Chem. 48: 125-149

Vyazovkin. S. V and Lesnikovich, A I, 1990. An approach to the solution of the inverse kinetic problem in the case of complex processes: Part 1. Methods employing a series of thermoanalytical curves Thermochim. Acta 165: 273-280.

Welham, N J, 2001. Enhanced dissolution of tantalite/columbite following milling, Int. J. Miner. Process. 61: 145-154.

Welham, N J, 2002. Activation of the carbothermic reduction of manganese ore, Int. J. Miner. Process. 67: 187-198.